Self-Limitation of Impurity Production by Radiation Cooling at the Edge of a Fusion Plasma

J. Neuhauser, K. Lackner, R. Wunderlich

IPP 1/198 April 1982

Reprint of ZEPHYR-Report No. 23 of April 1981.

IPP

MAX-PLANCK-INSTITUT FÜR PLASMAPHYSIK

8046 GARCHING BEI MÜNCHEN

MAX-PLANCK-INSTITUT FÜR PLASMAPHYSIK

GARCHING BEI MÜNCHEN

Self-Limitation of Impurity Production by Radiation Cooling at the Edge of a Fusion Plasma

J. Neuhauser, K. Lackner, R. Wunderlich

IPP 1/198 April 1982

Reprint of ZEPHYR-Report No. 23 of April 1981.

Die nachstehende Arbeit wurde im Rahmen des Vertrages zwischen dem Max-Planck-Institut für Plasmaphysik und der Europäischen Atomgemeinschaft über die Zusammenarbeit auf dem Gebiete der Plasmaphysik durchgeführt.

IPP 1/198

J. Neuhauser
K. Lackner
R. Wunderlich

Self-Limitation of Impurity Production by Radiation Cooling at the Edge of a Fusion Plasma

April 1982 (in English)

Abstract

The influence of radiation cooling at the edge of a fusion plasma on the plasma-wall interaction is numerically studied for parameters typical of the ZEPHYR ignition experiment. Various transport and impurity influx models and different external heating methods are studied using the 1D tokamak transport code BALDUR developed at Princeton. The results demonstrate the self-consistent formation of a radiating boundary layer (photosphere) for a wide range of parameters, limiting the impurity concentration in the plasma to a tolerable value. While the plasma behaviour is rather insensitive to model assumptions, the sputtering rate and the corresponding wall erosion depend on various parameters. Methods for external control of the photosphere and - more important - of the wall erosion are also discussed.

1. Introduction

At the high power level anticipated for ignition experiments or fusion reactors transport of the whole energy deposited in the plasma to the walls via particles would require particle energies far in excess of sputtering thresholds / 1 / and lead to a large impurity production rate.

As all considered impurity production mechanisms are driven, however, by high particle temperatures at the edge of the plasma (arcing, hydrogen and impurity ion sputtering) or its vicinity (sputtering by CX-neutrals) or spatial concentration of the charged particle heat flow (limiter damage) they should in principle have a self-limiting nature: the impurity concentration should saturate at a level, where the radiative losses from the plasma interior have reduced conductive and convective heat flow and the plasma temperature at the boundary to such a low level that the residual impurity sources just balance the diffusive impurity outflow.

The impurity content required for this equilibrium will depend on power flow, particle density, the radiation characteristics of the contaminant as well as on hydrogen and impurity ion density and heat conductivity profiles; it will only weakly depend on the detailed nature of the wall interaction model, which on the other hand will determine its accessibility and dynamics. By selecting the appropriate wall material its should be possible to get nearly 100 percent radiation at the boundary, while the centre remains unaffected by impurities.

The importance of radiation cooling of the plasma boundary was recognized very early and has been discussed in some detail by several authors /e.g. 2,3/.
Nevertheless, it seemed to be difficult to verify the basic ideas in existing 1D-tokamak transport codes. A first numerical indication for the existence of a cold plasma mantle was reported by Gibson /2,4 / for JET-extended parameters. Usually, however, the cold plasma mantle did not form spontaneously but a low energy neutral control beam was required to set it up and to maintain it. Even when the cold plasma mantle developed spontaneously during neutral injection, the low energy beam components seemed to be essential for its maintenance / 5 /.

Obviously, the question of the existence of a radiating stationary cold plasma mantle and its stability is not a trivial one, and the result may depend on various parameters / 4, 6, 7, 8, 9, 10 /. Especially in instationary phases with decreasing power flow from the plasma centre (e.g. end of heating pulse or shut-down) a radiation collapse of the whole plasma may occur. Another point is that too strong a cooling of the boundary layer might result in current peaking, sufficient to drive MHD instabilities.

In the present paper we reexamine the question of radiation cooling at the plasma edge by one-dimensional plasma simulations using the tokamak transport code BALDUR developed at Princeton / 11 /, and we demonstrate the existence of a self-sustained "photosphere" for a wide range of parameters, even in instationary phases. These computations were supported by analytic model calculations which yield simple scaling formulae for the most important quantities / 8 /.

Most of the simulations were done with central heating ("mock-up" ion cyclotron heating, α - heating etc.) of a plasma with high line density ($n \cdot a \gg 10^{15}$ cm^{-2}), i.e. the plasma radius a is much larger than the charge exchange length of thermal ions at density n. In this way a clear decoupling of the heating zone and the photosphere is achieved, a situation which is favourable for the formation of a cold plasma mantle and which, in addition, greatly simplifies the understanding of the most important physical processes related to the photosphere. First results for this scheme were reported in /8, 12/. Clearly, the situation is much worse in case of neutral injection heating, where the penetration depth of fast neutrals is not much higher than the charge exchange or ionization length of escaping thermal neutrals (except for extremely high neutral beam energy, e.g. from negative ion sources).

An important improvement was obtained by applying an analytical scrape-off layer model for the impurities / 13 /, which to lowest order simulates the shielding-out of impurities and, more important, the pumping of impurities by the limiter or divertor. The impurity pumping is essential during instationary phases, which require a decrease of the impurity content. Examples are, for instance, the end of the heating pulse (expecially with non-central heating methods, like neutral injection) or the shut-down procedure or merely the cooling phase of a thermonuclear burn-control cycle. First results with this improved model were presented in / 9 /.

In the following we first describe the specific transport, radiation and wall-interaction models used. Then we present the results obtained with parameters typical for ignition experiments like ZEPHYR and JET, assuming central heating (idealized ion cyclotron heating), which clearly demonstrate the self-limitation of impurities. The influence of the specific transport and wall-interaction models on the structure of the photosphere and its dynamics and on wall erosion will be discussed, including the option of an externally controlled impurity gas puff. We then consider the problems arising with neutral injection and/or adiabatic compressions. Finally we summarize the results by discussing three qualitatively different boundary structures and the conditions for their occurrence, including the general case with two or more impurities present simultaneously.

2. The Models Used in the 1D-Simulations

The one-dimensional tokamak transport code BALDUR / 11 /, which was used in our computations simulates essentially all the physical processes which are presently thought to be important for the particle and energy balance in tokamaks.

A variety of transport models can be chosen, others were added by us. Up to two impurity species can be handled. The average ion model is assumed for impurities and radiation is calculated from the corona model /14/.

An important part of the BALDUR-code is the Monte-Carlo neutral gas model, which allows for a fairly realistic description of gas puffing, recycling, neutral losses and charge-exchange sputtering of wall material. A detailed description of the code may be found in / 11 /.

Transport models:

Mostly, one of two transport models was used:

The standard transport model (I) is similar to the ALCATOR-INTOR model but with a different numerical factor:

Electron heat conduction: $\chi_e = 6.25 \times 10^{17} / n_e \; [cm^2/s]$

Ion heat conduction $\chi_i = 1 \times$ neoclassical

Particle diffusion $D = 0.2 \times \chi_e$ + neoclassical or 0

For typical ZEPHYR data it is slightly more pessimistic than the INTOR model.

As an alternate scaling law for χ_e (model II) which is sufficiently different from the standard model I we used a temperature dependent one as proposed in ref. /15/:

$$\chi_e = 8 \cdot 10^{13} \cdot \frac{B_t}{q(r)} \cdot \frac{a}{R} \cdot \frac{1}{nT} \left(\frac{n}{A} \right)^{1/5} \quad [cm^2/s]$$

(B [G], n [cm^{-3}], T [eV], A = atomic weight, q = safety factor). The temperature dependence is switched off below T_{min} by replacing $T \rightarrow (T^3 + T_{min}^3)^{1/3}$. Usually T_{min} = 270 eV is taken. The numerical factor is chosen consistent with PLT results, which indeed seem to indicate a temperature dependence of χ_e. An important point for ZEPHYR versus JET is the explicit dependence on the magnetic field strength which increases χ_e in high field machines but which is even less certain than the temperature dependence.

In addition, various modifications were tested, e.g. different numerical factors in model I or $\chi_e \sim (nT^{\gamma})^{-1}, 0 < \gamma \leq 1$ or $\chi_e \sim f(r)/n$, with f(r) increasing radially. Usually the neoclassical Ware pinch was included.

<u>Impurities and radiation model:</u>

The impurity studies were concentrated so far on iron as being typical for the intermediate Z materials, which have - at least in the coronal equilibrium model - the desireable characteristics to radiate predominantly in the boundary zone, at electron temperatures between several ten to several hundred eV. Low Z-materials would require higher impurity concentrations and would contribute to the shielding in case of the neutral injection beam, whereas high Z-ions would radiate strongly from the centre. Radiative losses were computed from the coronal equilibrium model. Finite rate effects would tend to shift the radiation maximum to higher temperatures, making lower-Z materials behave like the iron in the present calculations.

In a few runs the consequences of an additional puff of argon on the iron content was investigated.

Boundary condition at limiter radius r = a:

Hydrogen isotopes: $T(a) = T_{max}(a)$, $n(a) = n_{max}(a)$
for dT/dr, $dn/dr \leq 0$;
otherwise
$dT/dr(a) = 0$, $dn/dr(a) = 0$
with $T(a) < T_{max}(a)$, $n(a) < n_{max}(a)$

Iron impurity: net flux calculated using a 1D analytic scrape-off layer model (see below)

Argon impurity: flux prescribed (if used)

Wall interaction model:

The wall interaction model for iron includes sputtering of wall material by charge exchange neutrals (hydrogen isotopes), shielding and pumping by a scrape-off plasma layer in the limiter shadow (or a divertor scrape-off layer) and ion-sputtering by charged particles at the limiter, including impurity self-sputtering. Because of the poorly known physics, however, the latter is modelled in a rather crude way. Fig. 1 illustrates the different impurity fluxes:

The iron flux S_{cx} sputtered by charge exchange neutrals is ionized in the scrape-off and partly pumped by the limiter. Only part of it, $S_{cx} \cdot \exp(-d^*/\Delta)$, diffuses into the plasma. Δ is the scrape-off layer thickness and d^* denotes the average distance of the ionization zone from the plasma boundary (r = a).

The second source term is limiter sputtering, which we have, as a first approximation, coupled to the heat flux Q(a) onto the limiter minus a threshold value Q_{th}. The constant α_L is usually chosen such that the average particle energy required to conduct Q_{th} is of the order of 10 eV. It is zero if limiter sputtering is excluded (e.g. in a divertor tokamak).

These two influx terms are counteracted by the scrape-off layer pumping term which is proportional to the iron density $n_{Fe}(a)$ at the edge. The effective pumping speed, $\Delta/\tau_{\parallel}$, depends on the scrape-off layer geometry and the parallel flow time $\tau_{\parallel}$ to the limiter or divertor.

Details of the analytic 1-D scrape-off layer model and the derivation of d^*, Δ and $\tau_{\parallel}$ are described in / 13 /. The model is being improved, but it is felt that it contains already all the essential features governing the impurity dynamics.

3. Results Obtained With Central Heating

(a model ICRH-heating or α - heating)

3.1 Anomalous Plus Neoclassical Impurity Diffusion

(neoclassical temperature screening neglected)

As a first example, we simulate the heating scenario of a ZEPHYR-type ignition experiment with idealized ion cyclotron heating: the heating power is assumed to be deposited in a narrow vertical layer passing through the plasma centre (Fig. 2) and electrons and ions are assumed to be equally heated. The parameters chosen are: Major radius R = 1.35 m, minor radius a = 50 cm, toroidal magnetic field B_t = 9.14 T. The density is increased during heating up to final value of $n = 3.5 \times 10^{20}\ m^{-3}$. A 1 second heating pulse of only 11 MW is found to be sufficient to reach thermonuclear ignition in a deuterium-tritium plasma.

Because of iron sputtering at the wall and limiter, and because of rapid inward diffusion of iron through the hydrogen density gradient region (iron accumulation), the radiation in the boundary layer increases rapidly and a cold plasma mantle forms within several 100 milliseconds. It persists throughout the heating and the subsequent thermonuclear burning phase.

Fig. 3 shows typical temperature, density and heat flow profiles during the burn phase, 0.9 s after the end of the heating pulse.

Alpha heating occurs within 25 per cent of the plasma volume from where heat is conducted outward predominantly by electron heat conduction. In a narrow zone ("photosphere") of a few centimeters situated at about 90 per cent of the minor radius, this heat flow is converted into radiation, leaving a cold layer (several eV) in immediate contact with the limiter or walls.

Fig. 4 shows the time dependence of the most important parameters for the same case: An ohmic phase of 200 ms is followed by a 1 s heating pulse (11 MW deposited in the plasma). When the external heating power is switched off, the plasma profiles rearrange themselves according to the remaining, more centrally peaked α - particle heating and the temperature starts to run away. No burn-control is applied. The total toroidal beta at ignition including the α - particle pressure, is 2.3 per cent.

The bottom part of Fig. 4 shows the iron behaviour. According to the limiter sputtering coefficient α_L chosen, this sputtering term is dominant during the first few 100 ms and brings the iron concentration rapidly to about 0.05 per cent. The density on axis is delayed because of the finite inward diffusion time (no temperature screening). As the temperature at the boundary goes down the limiter sputtering decreases and charge-exchange sputtering remains, which decreases more slowly, according to the slowly growing thickness of the cold plasma mantle. Immediately after the end of the heating pulse the plasma mantle thickness increases rapidly for a short time, since the radiated power is higher than the heat flux from the centre. But after a slight rearrangement of the profiles in the boundary region (which occurs faster than global confinement times) an equilibrium state is reached, where the remaining sputtering flux is balanced by the limiter pumping as expected (Fig. 3 corresponds to t = 2.1 s). The transition from the heating to the burning phase is indeed critical and a slow decrease of the external power is advisable, in order to safely avoid a radiation collapse.

These results are by no means restricted to typical ZEPHYR parameters. If the same mock-up ion cyclotron heating is applied to JET or FED, we obtain very similar profiles except for the numerical values of density, power etc..

The sensitivity of the results with respect to changes in the limiter sputtering model was checked for ZEPHYR-parameters by changing the sputtering coefficient α_L between zero and 10 times the value chosen in the example described above. The result is summarized in Fig. 5 where the iron density on axis is shown as function of time with α_L as parameter (arb. units; $\alpha_L = 3.6$ is the standard case). We find that the iron concentration rises more rapidly with higher α_L, but that the final value is practically the same. Obviously, the saturation level is rather independent of the exact nature of the impurity production mechanism at material walls and this fact may justify a posteriori the choice of a rather crude limiter sputtering model.

Another check was made with respect to the anomalous part of the electron heat conduction and particle diffusion. Fig. 6 shows loss profiles for two representative cases, the first with an explicit radial dependence of the coefficient, increasing with the radius by one order of magnitude and the second with an inverse temperature dependence according to reference / 15 / (see also chap. 2). In both cases a slight distortion of the radiation profile is obtained, while the over-all structure remains unchanged. One should notice that, especially in the second case, the temperature and current profiles are rather peaked, a fact which could be a severe disadvantage of an otherwise optimistic transport law.

3.2 Anomalous Impurity Diffusion Only

If the impurity transport is assumed to be purely anomalous ($D = 0.2 \cdot \chi_e$) without any neoclassical contribution, then we obtain rather flat impurity profiles throughout the plasma in contrast to those shown in Fig. 3, where the iron density at the boundary is much lower than in the main plasma region. The consequence is that for equal iron concentration in the centre the impurity pumping rate of the scrape-off layer, which is proportional to the edge impurity density ($\phi_{pump} \sim n_{Fe}(a) \cdot \Delta / \tau_{\parallel}$) is much higher. This in turn means that a correspondingly higher impurity production rate at the walls can be tolerated and a cool plasma mantle may not be necessary to protect the plasma. (One should notice, however, that the wall erosion is then also much higher and a cool plasma mantle may be necessary in a stationary machine to protect the wall! This point of view will be discussed later on).

The numerical simulations demonstrate this behaviour clearly: For the ICRH-ZEPHYR data described above and $\alpha = 0$ the iron concentration saturates at $\lesssim 0.035$ per cent compared to $\lesssim 0.05$ per cent assuming impurity accumulation and no temperature screening. Only 50 to 60 per cent of the loss power is converted to radiation in the photosphere. The saturated iron sputtering rate caused by hot deuterium and tritium charge exchange neutrals is $\gtrsim 10^{15}\ cm^{-2}\ s^{-1}$ compared to $\sim 2 \times 10^{13}$ in the previous case.

Because of the large fraction of heat conduction at the boundary, the edge temperature remains high (an upper limit of 50 to 100 eV is usually set for T_e and T_i in the numerical simulations). $\alpha_L = 0$ would then be justified only in a divertor tokamak, where the limiter plasma interaction problem is shifted into a separate divertor chamber.

In a limiter tokamak like ZEPHYR or JET, a hot edge temperature causes a total limiter ion sputtering rate which is roughly of the same order of magnitude as the total charge exchange sputtering rate, if impurity self-sputtering is neglected. A corresponding case with $\alpha_L = 3.6$ is shown in Fig. 7 at $t = 1500$ ms. The only difference to Fig. 3 is the neglection of any neoclassical impurity transport in Fig. 7. The fraction of the power flow to the wall by heat conduction has reduced to about 14 per cent, and the charge exchange sputtering rate has decreased to $\lesssim 4 \times 10^{14}\ cm^{-2}\ s^{-1}$. Of course, the local limiter sputtering rate is much higher, if the limiter area is small, since the total rates are comparable!

Even in this case the edge temperature may be high enough to cause impurity self-sputtering. As long as the self-sputtering coefficient s is below unity, this can be accounted for by increasing the constant α_L by a factor $1/(1-s)$. For $s \gtrsim 1$ the impurity content would rapidly increase in time but the increasing radiation cooling would again restore $s < 1$. In this simple picture the temperature in the immediate neighbourhood of the limiter is expected to adjust itself close to the threshold value for self-sputtering of the limiter material (including acceleration effects in an electrostractic Debye-sheeth). Obviously, the detailed nature of the limiter sputtering mechanism is again of minor importance for the impurity content in the plasma.

With increasing α_L in the numerical simulations, the iron saturation value approaches again ~ 0.05 per cent, when the radiated power approaches 100 per cent. The total limiter and charge exchange sputtering rate is also well defined in equilibrium and is simply equal to the pumping rate of the scrape-off at that concentration (including those impurities which are directly pumped by the scrape-off without entering the central plasma). Therefore, increasing the pumping rate e.g. by reducing the distance between limiters would accordingly increase the total sputtering rate without much change in plasma parameters and iron concentration.

We note that at least for the specific example treated here a cool plasma mantle in the usual sense is not formed, since it is not necessary to suppress the hot charge exchange outflux. Only a rather narrow sheath close to the separatrix must be cooled down to the ion self-sputtering threshold.

3.3 The Effect of Neoclassical Temperature Screening

According to neoclassical theory the inward diffusion of impurities because of the hydrogen density gradient may reverse if the temperature gradient is much larger than the density gradient. Looking at the profiles of Fig. 3 we find that this is indeed the case in the central plasma, while in the edge region the density gradient is dominant. Therefore one would expect that temperature screening simply prevents the impurities from penetrating the centre, leaving the boundary layer (photosphere, cool plasma mantle) essentially unchanged.

Such an equilibrium would be even more favourable than that in Fig. 3, since radiation in the central plasma, which was already low, would be completely unimportant and the impurities would concentrate in that region where we would like to have them, in order to radiate away the power lost from the central plasma.

The actual structure, however, depends again on many parameters. For ZEPHYR data usually a thin photosphere close to the limiter radius is observed similar to that with anomalous impurity transport only. The impurities are concentrated in this cold layer while the centre if essentially clean.

3.4 Wall Erosion and External Control

We have already mentioned that without a cool plasma mantle of sufficient thickness the iron sputtering rate by charge exchange neutrals may be of the order of 10^{15} cm^{-2} s^{-1}, which for stainless steel would mean several millimeters of wall material per year in quasistationary operation (which was not aimed at in ZEPHYR, of course). An even much higher local sputtering rate is to be expected at the limiter in case of a high boundary temperature.

These values are not tolerable in a fusion reactor and even in future experiments the limiter loading may be critical. Therefore, if the impurity transport in future experiments turns out to be such that self-limitation of the wall erosion is not sufficient, then external control may be necessary. Additional requirements for external control may come from instationary phases, like shut-down of an ignited plasma without radiation collapse.

One possibility is to influence the electron heat conduction coefficient χ_e in the boundary layer, e.g. by external field line ergodization, as discussed elsewhere / 8 /. Increasing χ_e increases the total radiated power at a given impurity concentration. This is especially effective if the radiated power is already not too far from 100 per cent.

Another possibility is external impurity gas puffing. In this way it is possible to reduce the wall erosion to a tolerable level and to substitute the impurities from wall sputtering by externally controllable impurities. The type of impurity to be used can be chosen such as to optimize the external control of the photosphere (radiation characteristic, pumping efficiency for that gas etc.). As long as the wall material provides a substantial contribution to radiation in the photosphere, self-regulation within a reasonable interval is still to be expected. Otherwise a feed-back loop is necessary where the remaining hot charge exchange outflux could be used, for instance, as a measure for the control of the external impurity influx.

We demonstrate the interaction between internal and external impurity sources via the plasma boundary dynamics for the following example. We take conditions like those discussed in chap. 3.2 with $\alpha_L = 1$. Then the radiated fraction at the boundary is only $\lesssim 60$ per cent, the boundary temperature is high and the sputtering rate is around 10^{15} cm^{-2}s^{-1}. At t = 0.5 sec we start to puff argon at a constant average rate of $5 \cdot 10^{13}$ cm^{-2}s^{-1} (without any pumping of argon for convenience). The total radiation then increases because of the increasing argon contribution and a cold plasma mantle starts to develop. The limiter sputtering and lateron also the charge exchange sputtering decrease. Because of iron pumping by the scrape-off the iron concentration also begins to decrease.

As a result, iron is effectively substituted by argon and the wall erosion is reduced by more than one order of magnitude. Fig. 8 shows the iron and argon concentrations as function of time compared to the case without argon.

4. Results with Neutral Injection and Adiabatic Compression

In the preceeding chapter we have seen that in case of a sufficiently central heat deposition a photosphere is formed spontaneously (or can be set up or manipulated by external means) for a wide range of parameters. Indeed, the most important type of heating in a stationary or quasistationary fusion reactor, namely the thermonuclear α - heating, is strongly peaked to the centre and therefore the ideas described above should well apply to the thermonuclear bum phase.

A different situation is to be expected during the initial heating phase, and, perhaps more important, in a driven mode of operation, if a heating method with a noncentral heat deposition is applied. Unfortunately, the neutral injection as foreseen for ZEPHYR, JET and other fusion test experiments is of that type. On one side, the ignition condition $n\tau_E > 2 \times 10^{14}\ cm^{-3}s$ is also a condition for the line density na > $(na)_{crit}$, if empirical scaling is assumed ($\tau_E \sim na^2$). On the other side, positive ion technology does not allow for beam energies far above 160 keV, as would be necessary to penetrate those plasmas.

As a consequence, the photosphere is no longer decoupled from the heating zone, and the energy balance in the boundary layer is appreciably changed. Self-limitation of impurities may be impossible, or, at least, much more impurities may be produced during neutral injection than can be tolerated in the subsequent burn phase.

Another problem occurs in connection with adiabatic major radius compression as in the ZEPHYR standard design. If the radiation power from the photosphere is already nearly 100 per cent of the total loss power, then the plasma suffers a radiation collapse during or after adiabatic compressions, since the radiation increases more rapidly than the total loss power during the radial inward motion.

The numerical simulations show that both effects pose some restrictions on the standard heating scenario of ZEPHYR which is a combination of a one second neutral injection pulse with a subsequent major radius compression ($R_1/R_2 = 1.5$). During neutral injection appreciably more iron impurities are produced than with central heating (up to several per mille, depending on the impurity model assumed). Because of the short injection pulse, however, the deleterious effects are not too severe. The main problem arises during adiabatic compression: as stated earlier, an impurity transport model which leads to the desired spontaneous formation of a cold plasma mantle during neutral injection, is completely undesireable in connection with compression and will result in a radiation collapse.

On the other side, if only anomalous impurity transport is taken and if impurity self-sputtering at the limiter is low enough, then no prohibitive effects occur. An example is presented in Fig. 9 including the most important data.

The temperatures, beta and the iron content are shown as functions of time. We note that the neutral injection is kept on during adiabatic compression, since otherwise a faster compression speed would be required which is technically difficult because of the finite vertical field penetration time through the main field coils.

It is instructive to compare the average iron concentration and the iron density on axis in Fig. 9 with those values given in Fig. 4. Despite the more optimistic iron transport in Fig. 9 the iron concentration increases rapidly to ~ 0.2 per cent. After the end of the heating phase, the concentration drops again. Provided that some type of burn control were active, it would asymptotically approach ~ 0.03 per cent as found for central heating in that case. We also emphasize that $\beta \approx 3.1$ per cent immediately after heating, while the asymptotic value, again with active burn control, would be below 2.3 per cent.

So, an indirect consequence of the heating dynamics including impurities is that the beta requirements (MHD-stability!) are higher with noncentral heating. A design adequate for the initial phase would be unnecessarily safe during the burn-phase, which in an ignited reactor is hopefully nearly 100 per cent of cycle.

An interesting question is what happens if neutral injection is applied without compression like in JET, INTOR etc.. For that case we have made several preliminary runs simulating JET / 16 / and FED and the results are as follows:

With anomalous impurity transport only the iron pumping through the scrape-off layer is sufficient to keep the impurity content at a level which is just tolerable. A cold plasma mantle is not observed and the question of impurity self-sputtering remains as discussed.

If impurity accumulation is included, but not temperature screening, then shortly after switching on the neutral beam a fairly cool plasma mantle develops with slowly increasing width. The temperature in this region (several tens eV) is not low enough to substantially reduce the iron sputtering and the self-limitation does not work. Therefore the impurity content continues to increase, the hot plasma shrinks and the plasma suffers a radiation collapse before ignition temperatures are reached. Only for the rather optimistic transport model II ignition in an elliptical JET-plasma may be possible inspite of impurity accumulation because of the lower neutral injection power necessary for heating to ignition in this case. Less problems are expected if outward driving effects like temperature screening are included.

5. Discussion of Results

The large variety of model assumptions and results described in the preceeding paragraphs simply reflects the present uncertainty with respect to energy and particle (especially impurity) transport in the central plasma and the detailed nature of plasma-wall interaction in the edge region. Because of this uncertainty it is impossible to predict the impurity behaviour in future experiments with the desired accuracy. There are, however, general features which can be derived from our simulations.

For simplicity, the discussion will be restricted to central heating and therefore clear decoupling of the heating zone and the boundary layer. As mentioned, the thermonuclear burn phase (α - heating) in an ignited reactor is certainly of this type. In addition, impurities (wall material) with appropriate radiation characteristic are chosen as discussed earlier. What are then the conditions for the existence of a photosphere or, in addition, a cool plasma mantle and how large is the corresponding wall erosion?

Obviously, an important question is that of impurity transport which influences the impurity density and radiation profile. A second important quantity is the impurity pumping rate which is proportional to the impurity density at the separatrix and depends on the limiter or divertor geometry and on the transport in the scrape-off layer. Finally, we need the impurity production rate which depends on the plasma boundary parameters (external sources and fusion products are not considered for the moment). All three together determine the absolute impurity content and the radiation profile. (Of course, the electron and hydrogen density and temperature profiles are equally important, but we focus our attention on the impurity data for this discussion). As a further simplification the internal transport and the pumping by the scrape-off may be represented by a global impurity confinement time.

It is then useful to distinguish three regimes according to different parameters in the boundary layer:

(1) A hot boundary may be expected for very low iron confinement time (high pumping efficiency; high anomalous impurity diffusion, eventually including an additional outward term like "temperature screening" etc.).

The impurity concentration is then low and radiation is unimportant throughout the plasma.

We emphasize that this state is extremely unlikely in a limiter tokamak like JET or ZEPHYR, since an excessive impurity self-sputtering at the limiter would rapidly increase the impurity content, creating a layer as described below. In a divertor tokamak, however, a hot boundary may be feasible, since the limiter problem is transferred to a separate chamber and decoupled from the main plasma. On the other side, the remaining wall erosion may be too high for a reactor (full charge exchange sputtering).

(2) A thin cold surface layer is expected for intermediate confinement time and moderate limiter sputtering coefficient, but also for low confinement time in case of a high limiter sputtering coefficient. The ion temperature will be close to the threshold for limiter sputtering (hydrogen or impurity self-sputtering depending on actual numbers) and the radiated power at the boundary is nearly 100 per cent of the total loss power.

The equilibrium is selfregulating in the sense that an increasing impurity concentration will be counteracted by a decrease in the limiter sputtering rate via radiation cooling and vice versa. The detailed nature of limiter-plasma interaction is not important.

The limiter erosion is the higher the lower the impurity confinement time is. This means that low pumping speed and/or impurity accumulation are favourable for low limiter erosion! The wall erosion by charge exchange neutrals is essentially unaffected by the thin layer ($n \cdot \delta \ll 2 \times 10^{15}\ cm^{-2}$) and may again be untolerable in a stationary machine (δ is the width of the cool layer).

(3) A cool plasma mantle with $n \cdot \delta \gtrsim 2 \cdot 10^{15}\ cm^{-2}$ is expected for high impurity confinement time (e.g. moderate anomalous diffusion plus neoclassical accumulation, at least in the boundary region). A nearly complete conversion of heat flux into radiation occurs further in the plasma and the cool mantle is thick enough to reabsorb most of the hydrogen charge exchange neutrals from the hot interior. Limiter sputtering is essentially switched off. The remaining charge exchange sputtering depends on the actual confinement time of impurities, but usually the corresponding wall erosion will be small and tolerable.

Again the equilibrium is self-adjusting in the sense that now the charge exchange sputtering is controlled by an appropriate readjustment of the mantle thickness δ.

In case (2) and (3) a "photosphere" is established, that means there is a layer where the energy flux is converted into radiation. In (2) this layer lies close to the flux surface touching the limiter, while in (3) it is located at the inner boundary of the cool plasma mantle. A fraction of the total radiation flux originates also from the central plasma as can be seen in Fig. 3. An important question which has not yet been finally answered is the stability of such radiation layers /e.g. 6,7,8,5/, though the numerical simulations would indicate the existence of stable solutions.

Starting from the simple cases discussed above one may now try to analyse more complex situations, like non-central heating or instationary phases (e.g. shut down) or the interaction between two or more impurities.

The latter case is certainly important in any experiment and may be important for external control. Obviously, in case of very low impurity confinement time, the contributions of individual impurity species simply add up, as long as the total radiation is unimportant for the energy balance ("linear" range). When the total radiated power, however, approaches 100 per cent, then a strong interaction via self-regulating mechanisms occurs ("non-linear" range). Following the interpretation given above ((2) + (3)), it is expected that the impurity with the lowest threshold will be the dominant one, while the production of other impurities may be nearly switched off. This may change only, if the effective confinement time of individual impurities is very different (e.g. low pumping rate, i.e. high recycling for rare gases). The interaction with externally puffed impurities for control has already been discussed in paragraph (3.4).

Finally, we note that radiation may not be the only cooling mechanism in the boundary. Charge exchange neutrals and hydrogen ionization and radiation could also carry an important fraction of the energy flux. These effects are included in our simulations but turn out to be of minor importance for the parameter range studied hitherto.

Conclusions

Radiation cooling of the plasma boundary (a "photosphere") has been postulated in the literature as a solution for the power transfer to the walls in large fusion machines.

In a series of 1D-plasma simulations (Princeton BALDUR-code) mostly for the ZEPHYR ignition experiment we have examined the compatibility of such conditions with self-consistent wall interaction models and different electron heat conduction laws and auxiliary heating methods.

The studies were concentrated on iron impurities as being typical for the intermediate Z materials, which have the desirable characteristics of radiating predominantly in the boundary zone (< 1 keV).

For central heating methods (a model ICRH deposition profile or α- particle heating) stationary equilibria with effective radiation cooling at the boundary are estabilished over a wide range of model assumptions. Because of self-limitation, the impurity content in the plasma remains at a tolerable value in all cases, that means that the impurity problem is not a serious one for the plasma itself! The impurity production rate at the walls and the corresponding wall erosion, however, are strongly dependent on the efficiency of impurity pumping by the limiter or divertor and the impurity transport in the plasma (i.e. on the effective impurity confinement time).

On the other hand, a badly penetrating neutral injection heating (either direct or in combination with adiabatic compression) requires careful choice of the scenarios and is compatible only with certain impurity transport models.

As an example for external control of the photosphere and wall erosion we have shown that by an appropriately timed argon puff in a burning plasma iron can be driven out of the plasma and an initially high wall erosion can be lowered to an acceptable level.

Acknowledgements

We are grateful to the Princeton BALDUR group for providing their numerical code. We also thank Dr. K. Borrass for his cooperation concerning his analytic scrape-off model, A. McKenny for various improvements of the BALDUR-code and Dr. W. Schneider for his assistance concerning the CRAY Version and boundary conditions.

References

/1/ H. Kotzlowski, F. Mast, H. Vernickel, 4th Int. Conf. on Plasma Surface Interaction in Contr. Fusion Devices, Garmisch-Partenkirchen, Germany, April 1980 (to be published in J. Nucl Mat. 94 & 95 (1980)

/2/ A. Gibson, J. Nucl.Mat. 76 & 77, 92 (1978)

/3/ Y. Shimomura, Nucl. Fus. 17, 626 and 1377 (1977)

/4/ M.L. Watkins, A. Gibson, 8th Europ. Conf. on Controlled Fusion and Plasma Physics (Prague, 1977), Vol. 1, p. 31 (1977)

/5/ M.L. Watkins et al., Brussels (1980), CN 38/W-3, Proceedings to be published by IAEA, Vienna

/6/ P.H. Rebut, B.J.Green, Plasma Physics and Contr. Nucl. Fusion Research 1976; Vo. II, p. 3, IAEA Vienna (1977)

/7/ N. Ohyabu, Nucl. Fusion 19, 1491 (1979)

/8/ J. Neuhauser, Report IPP 1/182, Garching, Aug. 1980

/9/ J. Neuhauser, K. Borrass, K. Lackner, L. Lengyel, W. Schneider, R. Wunderlich, Bull.Am.Phys.Soc. 25, 1039 (1980)

/10/ D.E.T.F.Ashby, M.H. Hughes, Bull.Am.Phys.Soc. 25, 1032 (1980)

/11/ BALDUR: A One-Dimensional Plasma Transport Code by D. Post, C. Singer, D.Mikkelsen, A. Silverman, F. Seidl, P.Rutherford, R.Hawryluk, A.McKenney L. Foote, D. Heifetz, W. Houlberg, M. Hughes, R. Jensen, G. Lister and J. Odgen

A description of BALDUR is presented in:

D.E. Post, C.E. Singer, A. McKenney and the PPPL Transport Group: "Working Draft of the BALDUR Documentation", TFTR Physics Group Report # 33, Princeton Plasma Physics Laboratory, January 1981

Note: The results presented in the present report were obtained using a version of BALDUR obtained from the PPPL transport group in 1980 (without numerical scrape-off region). At present we use the version BALDIØ7R (implemented at the Garching CRAY by C.E.Singer during a short visit); if operated without numerical scrape-off the results are the same as before.

In both cases the original neutral gas monte carlo routine was replaced by a vectorized version, written by A.McKenney at IPP.

/12/ O. Gruber, K. Lackner, J. Neuhauser, W. Schneider, R. Wunderlich, Heating of Toroidal Plasmas, Como, Italy, Sept. 1980, Paper C 48 (proceedings to be published)

/13/ K. Borrass, Report IPP 4/191, Garching, Aug. 1980

/14/ D.E. Post et al., Atomic Data and Nucl. Data Tables, Vol. 20, 397 (1977)

/15/ B. Coppi, E. Mazzucato, Phys. Letters 71 A, 337 (1979)

/16/ J. Neuhauser, K. Borrass, K. Lackner, R. Wunderlich, "Conditions for the Existence of a Stable Photosphere at the Edge of a Hot Plasma"; JET Workshop on 1D Transport Codes and Scrape-off Layers, Feb. 24-25, 1981

Figure Captions

Fig. 1 Wall interaction model and the corresponding fluxes at limiter radius calculated from the analytic scrape-off layer model /13/.

Fig. 2 Heat deposition profile modelling idealized ion cyclotron resonance heating (CIRH)

Fig. 3 Temperature, density and heat flow profiles for an "ICRH"heated ZEPHYR-type plasma, assuming anomalous impurity transport plus neoclassical accumulation, but without temperature screening (t = 2100 ms, see Fig. 4).
The heating and loss powers given are integrated over the volume with radius r. ALF and OHM mean α - and ohmic heating. ELE, ION, RAD and CX refer to transport by electrons, ions, radiation and charge exchange neutrals, respectively.

Fig. 4 Time dependence of plasma parameters in the heating and α - burning phase in a ZEPHYR-type plasma with "ICRH", assuming neoclassical impurity accumulation without temperature screening.
In the upper part we show peak and average density and temperatures and the total beta, the poloidal beta and the α - contribution to the total beta.
The lower part shows the time evolution of the iron concentration C_{Fe}, the iron density on axis, and the iron influx. The saturation effect is clearly demonstrated. The profiles in Fig. 3 are taken at t = 2100 ms.

Fig. 5 Iron density on axis for different limiter sputtering constant α_L; other data similar to the case shown in Figs. 3 + 4. While the typical rise time decreases with increasing α_L , the saturation level is nearly independent of it.

Fig. 6 Loss power profiles for different anomalous contribution to the electron heat conduction and the particle diffusivities (abbreviations see Fig. 3).

Top: $\chi_e = 2 \cdot 10^{17} / \{ n_e [(1 - r^2/a^2)^{3.5} + 0.1] \}$;

Bottom: $\chi_e = 8 \cdot 10^{13} B_t \cdot a (n / A)^{0.2} / \{ q(r) R n T \}$ (model II).

In both cases χ_i = noeclassical; D_H, $D_{Fe} = 0.2 \chi_e$ + neoclassical accumulation terms (without temperature screening).

Fig. 7 Temperature, density and heat flow profiles for an "ICRH"-ZEPHYR plasma as shown in Fig. 3, but now with only anomalous impurity transport (t = 1500 ms). In contrast to Fig. 3 the iron profile is now flat in the boundary layer and no cool plasma mantle has developed (for abbreviations see Fig. 3).

Fig. 8 Interaction between two types of impurities. If argon is puffed externally, the iron sputtering rate and as a consequence the iron concentration C_{Fe} decreases appreciably, when the radiated power approaches 100 per cent of the total loss power.

Fig. 9 Time dependence of plasma parameters for the ZEPHYR standard heating scenario (only anomalous iron transport; $\alpha_L = 1$). In comparison with the "ICRH" ZEPHYR case presented in Fig. 4, we see that the iron concentration C_{Fe} reaches a much higher level during neutral injection, despite the neglection of neoclassical impurity accumulation.

(Neutral injection: 20 MW (total), 160 keV-system.

Adiabatic compression: $R_1 = 202.5$ cm, $R_2 = 135$ cm.

The final plasma geometry is identical to that used for the "ICRH" ZEPHYR.)

Fig. 1

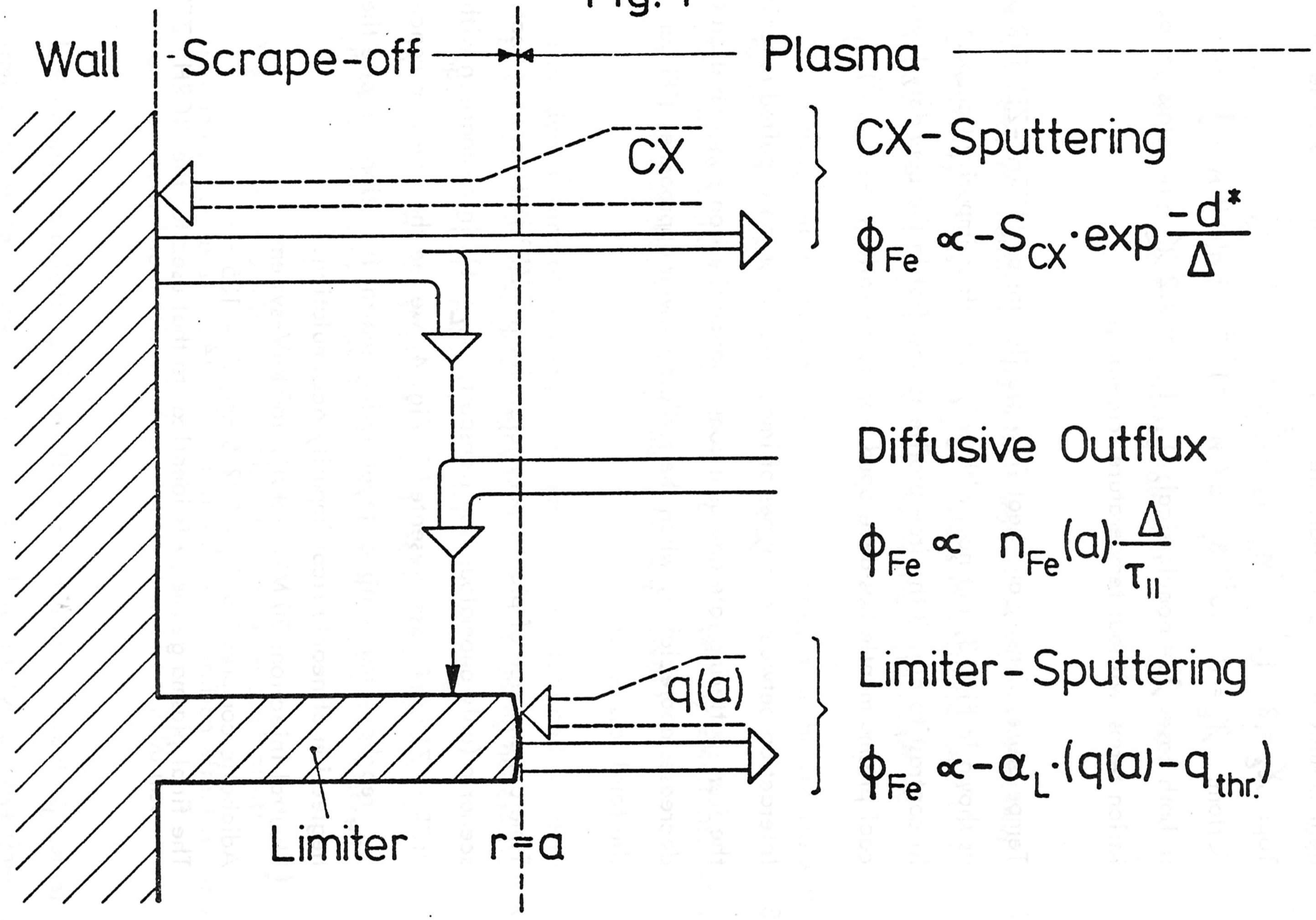
Wall
Scrape-off
Plasma
CX
CX - Sputtering
$\phi_{Fe} \propto -S_{CX} \cdot \exp \frac{-d^*}{\Delta}$
Diffusive Outflux
$\phi_{Fe} \propto n_{Fe}(a) \cdot \frac{\Delta}{\tau_{\parallel}}$
q(a)
Limiter - Sputtering
$\phi_{Fe} \propto -\alpha_L \cdot (q(a) - q_{thr.})$
Limiter
r = a

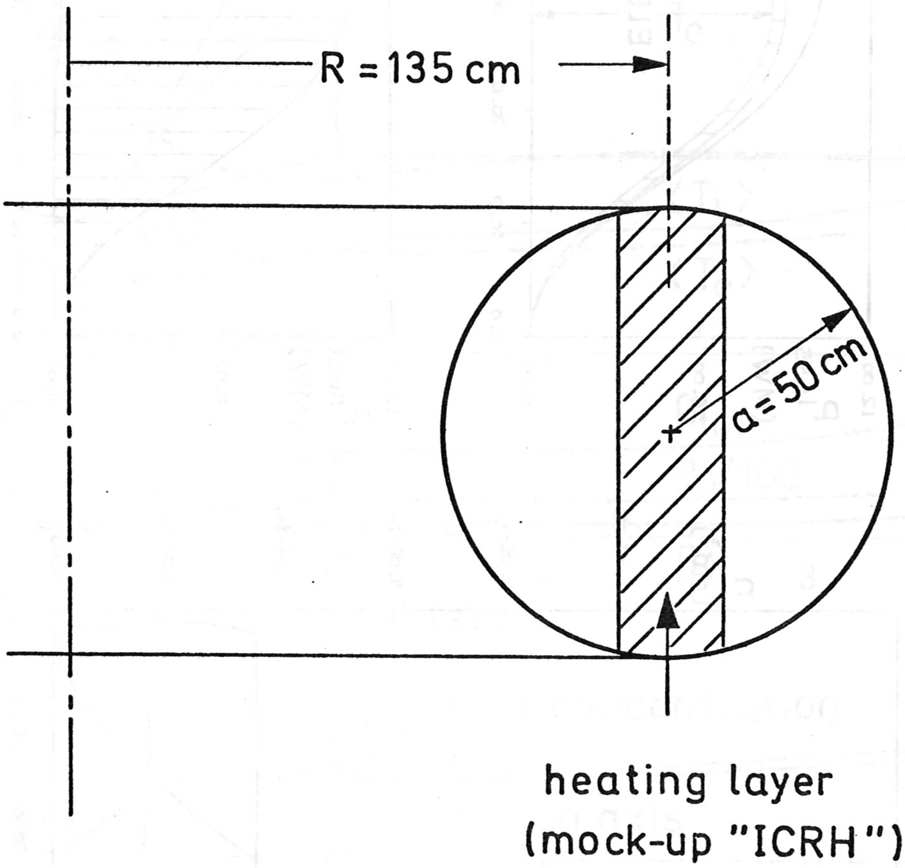

Fig. 2

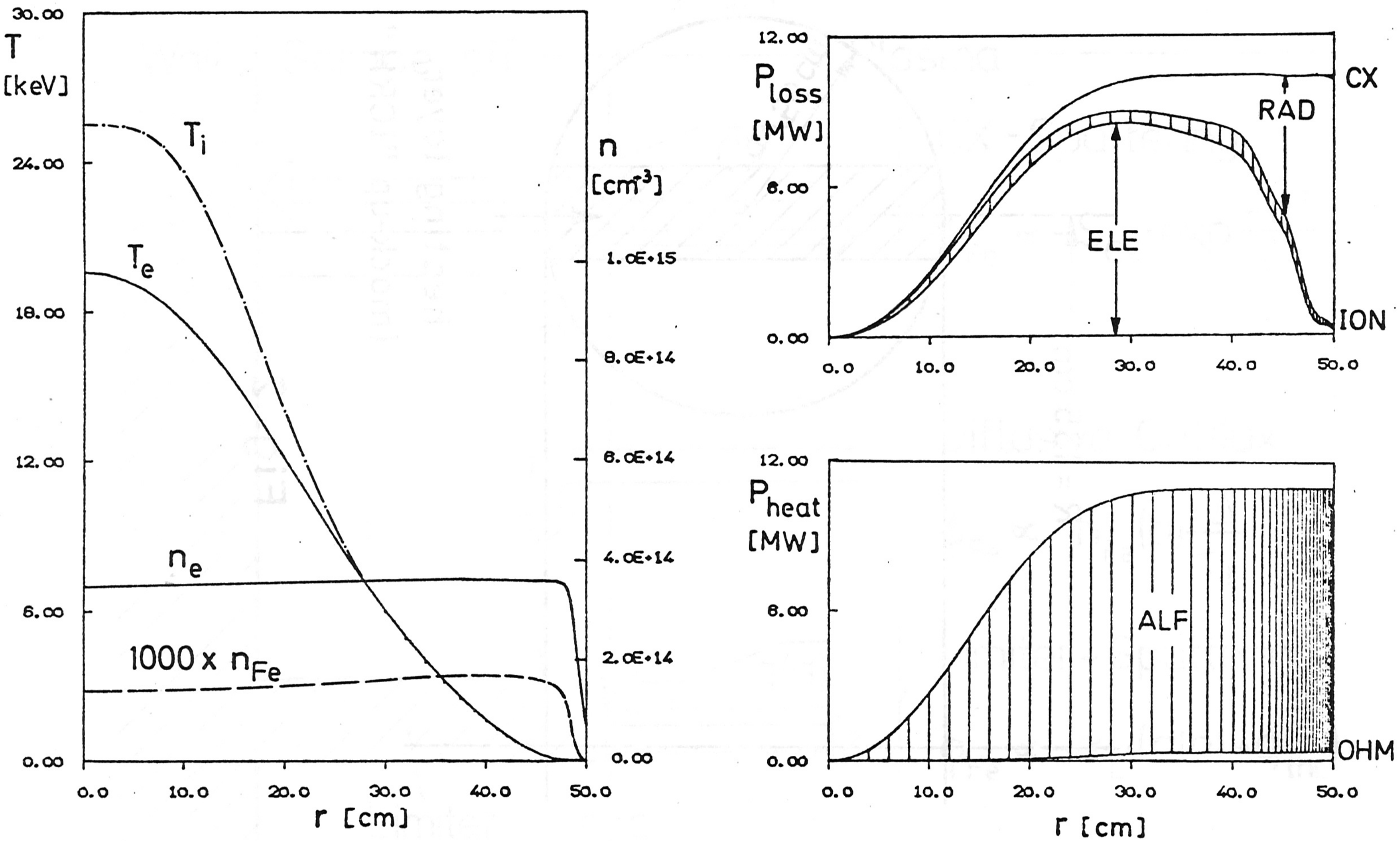
T
[keV]
30.00
24.00
18.00
12.00
6.00
0.00
T_i
T_e
n_e
1000 x n_Fe
n
[cm^-3]
1.0E+15
8.0E+14
6.0E+14
4.0E+14
2.0E+14
0.00
0.0
10.0
20.0
30.0
40.0
50.0
r [cm]
P_loss
[MW]
12.00
6.00
0.00
CX
RAD
ELE
ION
P_heat
[MW]
ALF
OHM

Fig. 3

Fig. 4

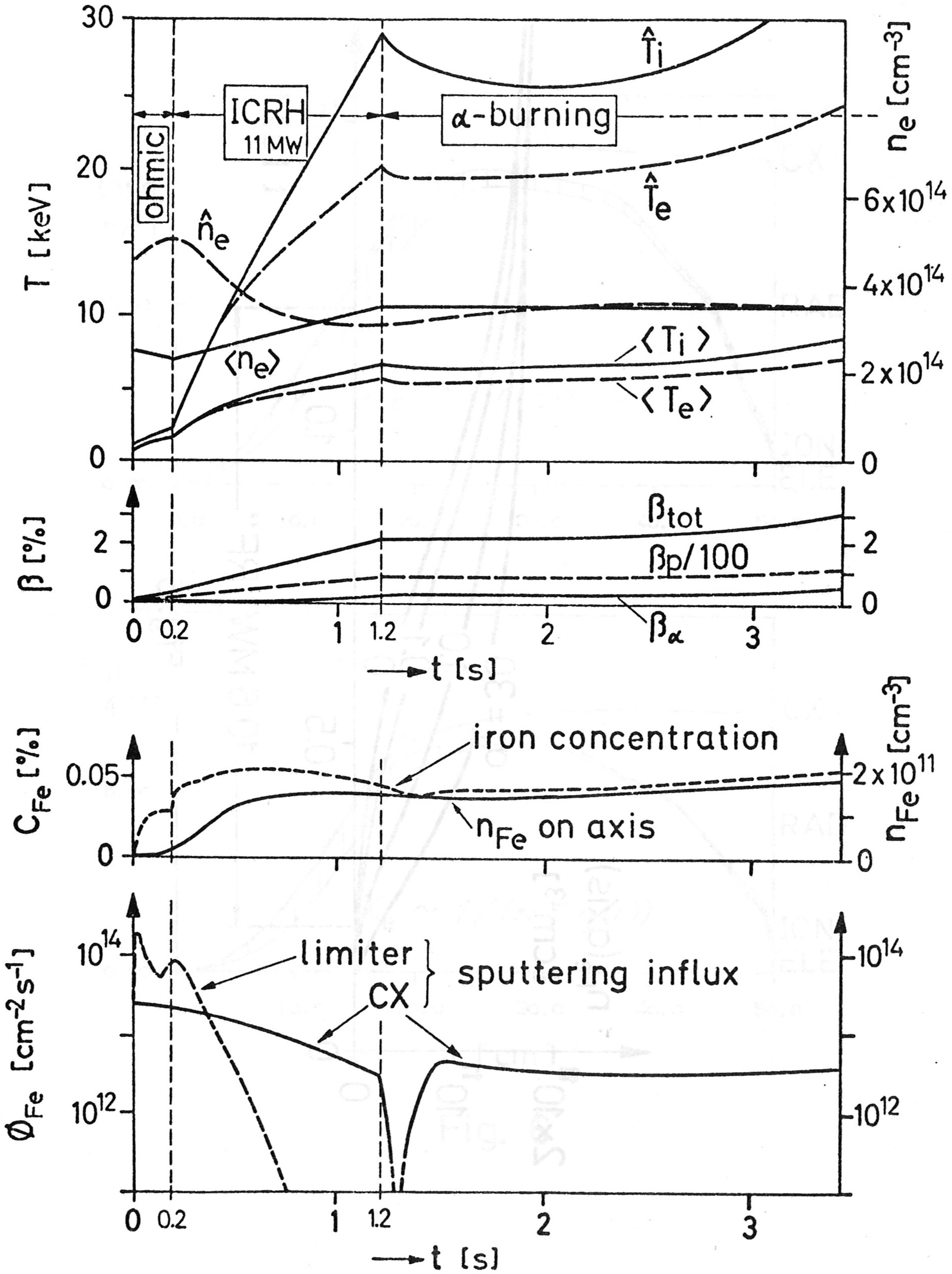

30
20
10
0
T [keV]
$\hat{T}_i$
ICRH
11 MW
α-burning
ohmic
$\hat{T}_e$
$\hat{n}_e$
$\langle n_e \rangle$
$\langle T_i \rangle$
$\langle T_e \rangle$
n_e [cm^{-3}]
6x10^{14}
4x10^{14}
2x10^{14}
β [%]
β_{tot}
$\beta_p/100$
β_α
0 0.2 1 1.2 2 3
t [s]
C_{Fe} [%]
0.05
iron concentration
n_{Fe} on axis
2x10^{11}
n_{Fe} [cm^{-3}]
Φ_{Fe} [cm^{-2}s^{-1}]
10^{14}
10^{12}
limiter
CX
sputtering influx
t [s]

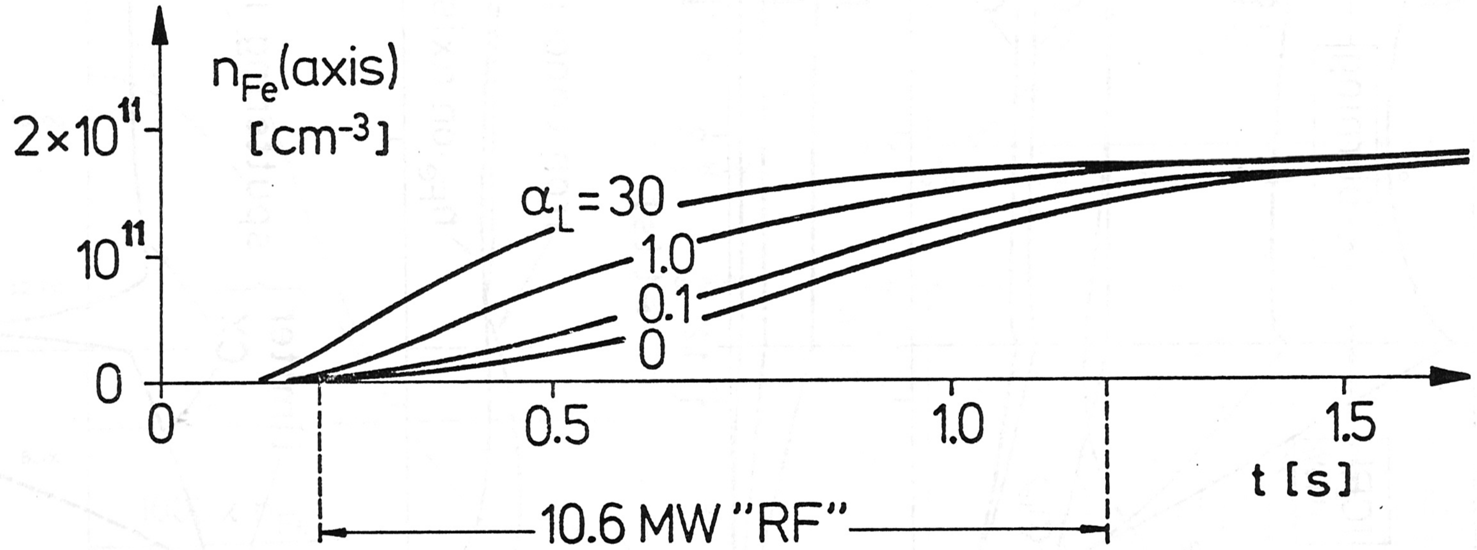
n_{Fe}(axis)
[cm^{-3}]
2×10^{11}
10^{11}
0
$\alpha_L = 30$
1.0
0.1
0
0
0.5
1.0
1.5
t [s]
10.6 MW "RF"

Fig. 5

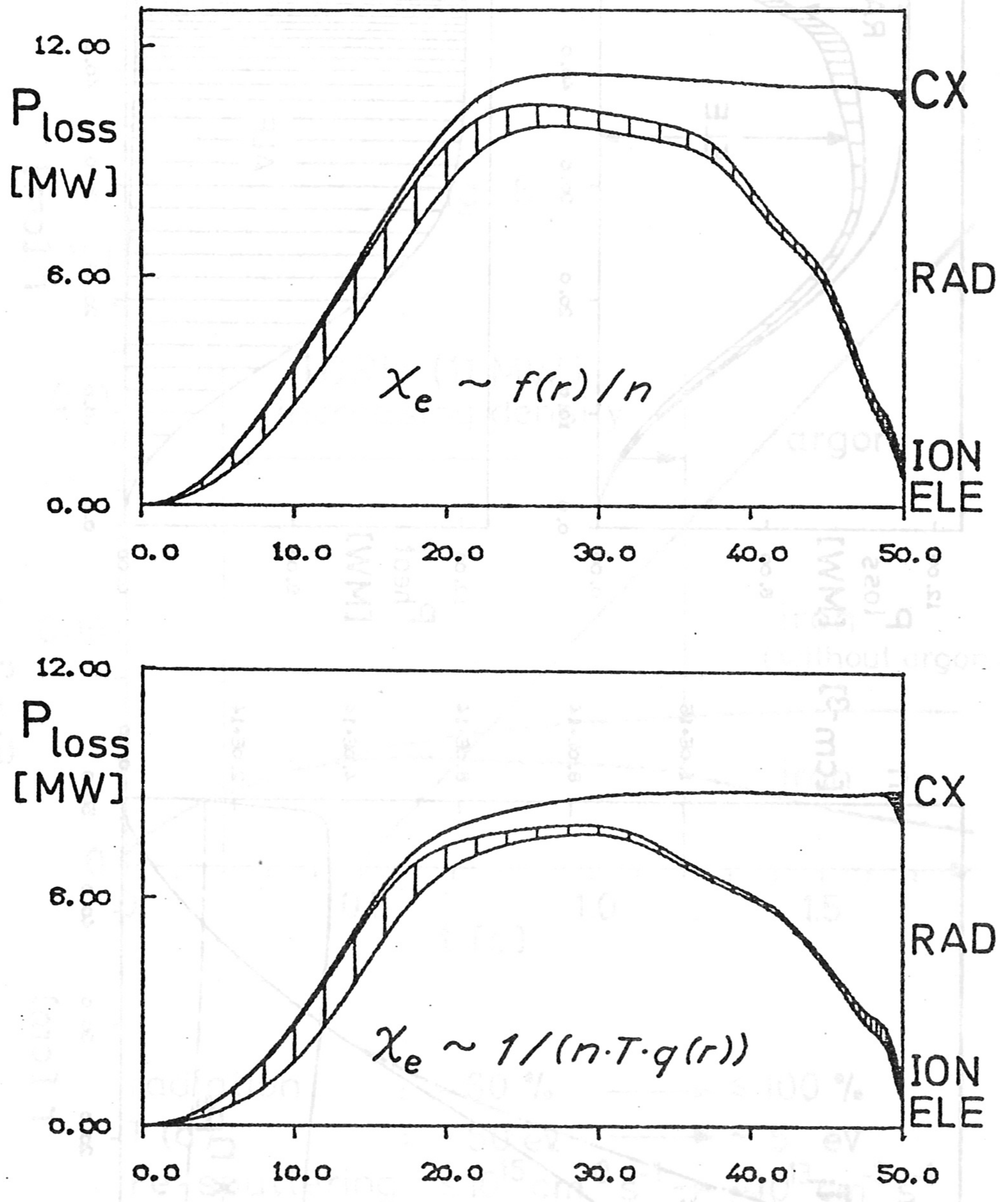

12.00
P_{loss}
[MW]
6.00
0.00
CX
RAD
ION
ELE
$\chi_e \sim f(r)/n$
0.0
10.0
20.0
30.0
40.0
50.0
12.00
P_{loss}
[MW]
6.00
0.00
CX
RAD
ION
ELE
$\chi_e \sim 1/(n \cdot T \cdot q(r))$
0.0
10.0
20.0
30.0
40.0
50.0
r [cm]

Fig. 6

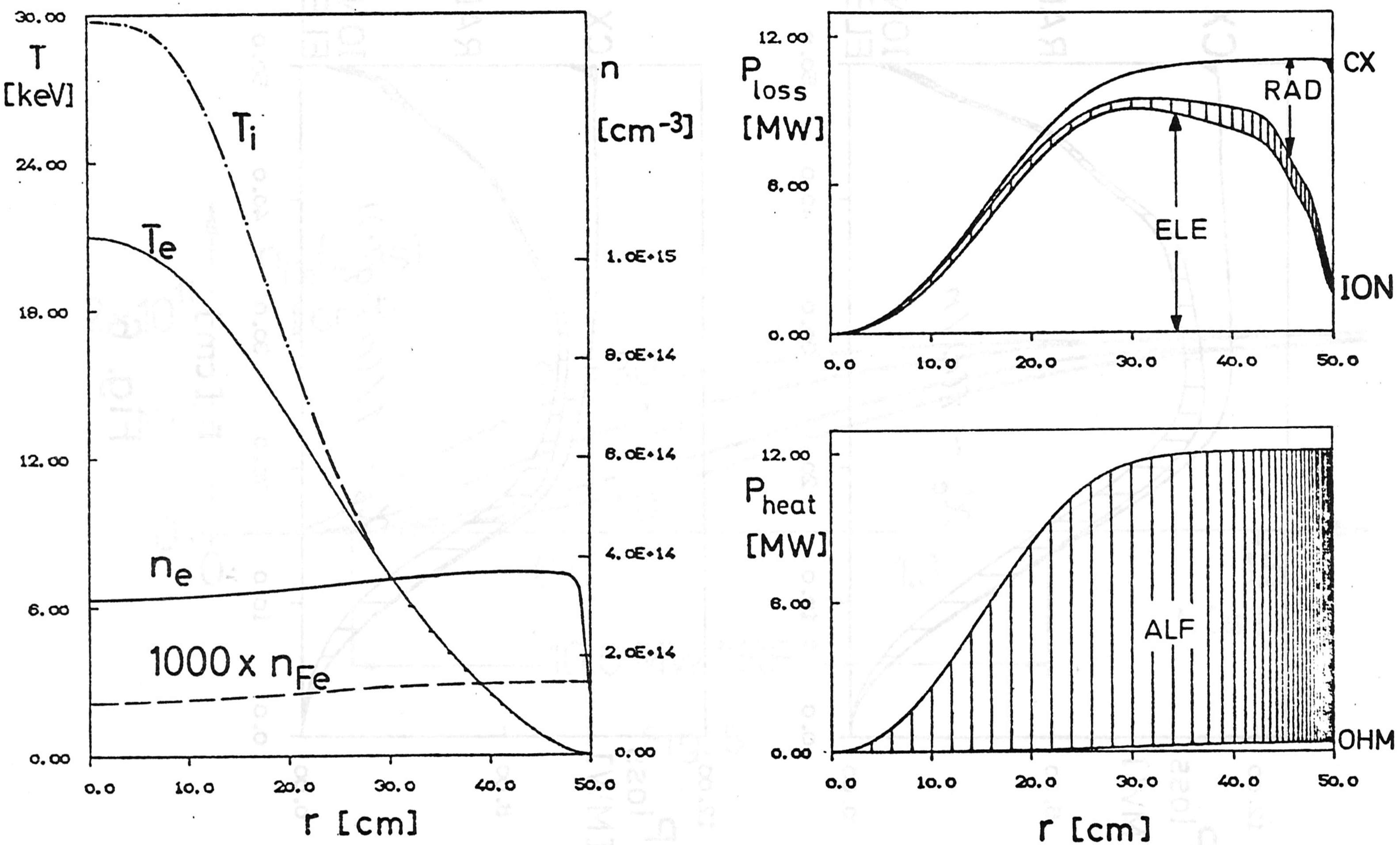
30.00
T
[keV]
24.00
18.00
12.00
6.00
0.00
T_i
T_e
n_e
$1000 \times n_{Fe}$
n
[cm^{-3}]
1.0E+15
8.0E+14
6.0E+14
4.0E+14
2.0E+14
0.00
0.0
10.0
20.0
30.0
40.0
50.0
r [cm]
12.00
P_{loss}
[MW]
6.00
0.00
CX
RAD
ELE
ION
P_{heat}
[MW]
ALF
OHM
r [cm]

Fig.7

Fig. 8

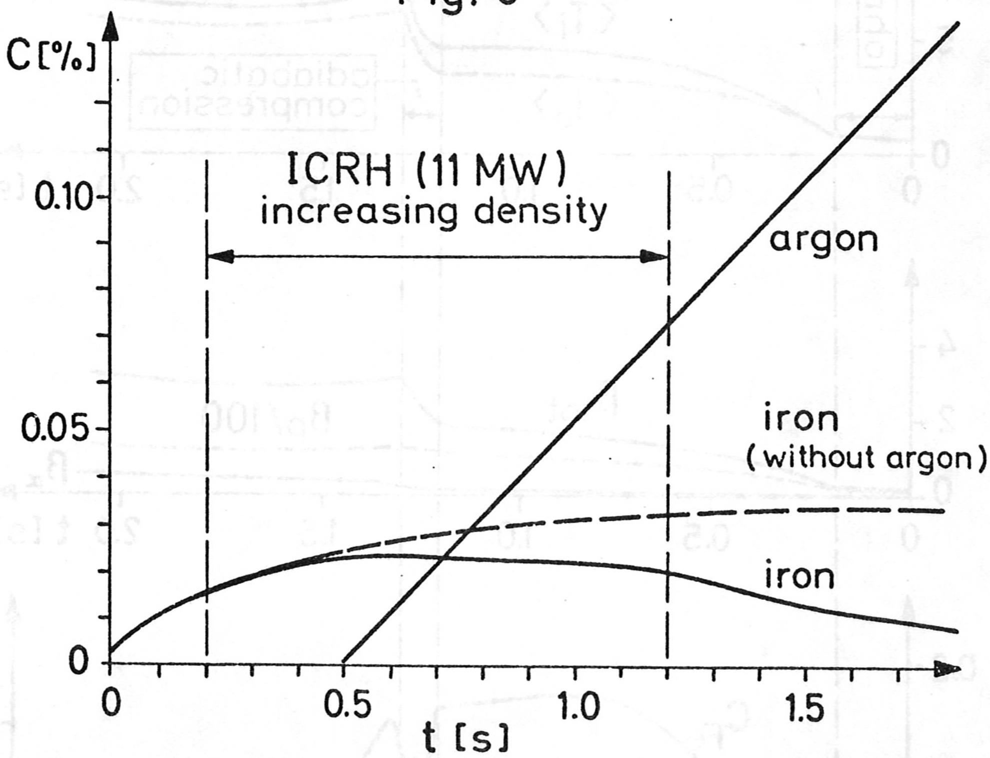

radiation : ~ 60 % → ≲ 100 %

T (a) : ~ 50 eV → ~ 5 eV

Fe-sputtering: ≲ 10^{15} cm^{-2} s^{-1} → ~10^{13} cm^{-2} s^{-1}

Fig. 9

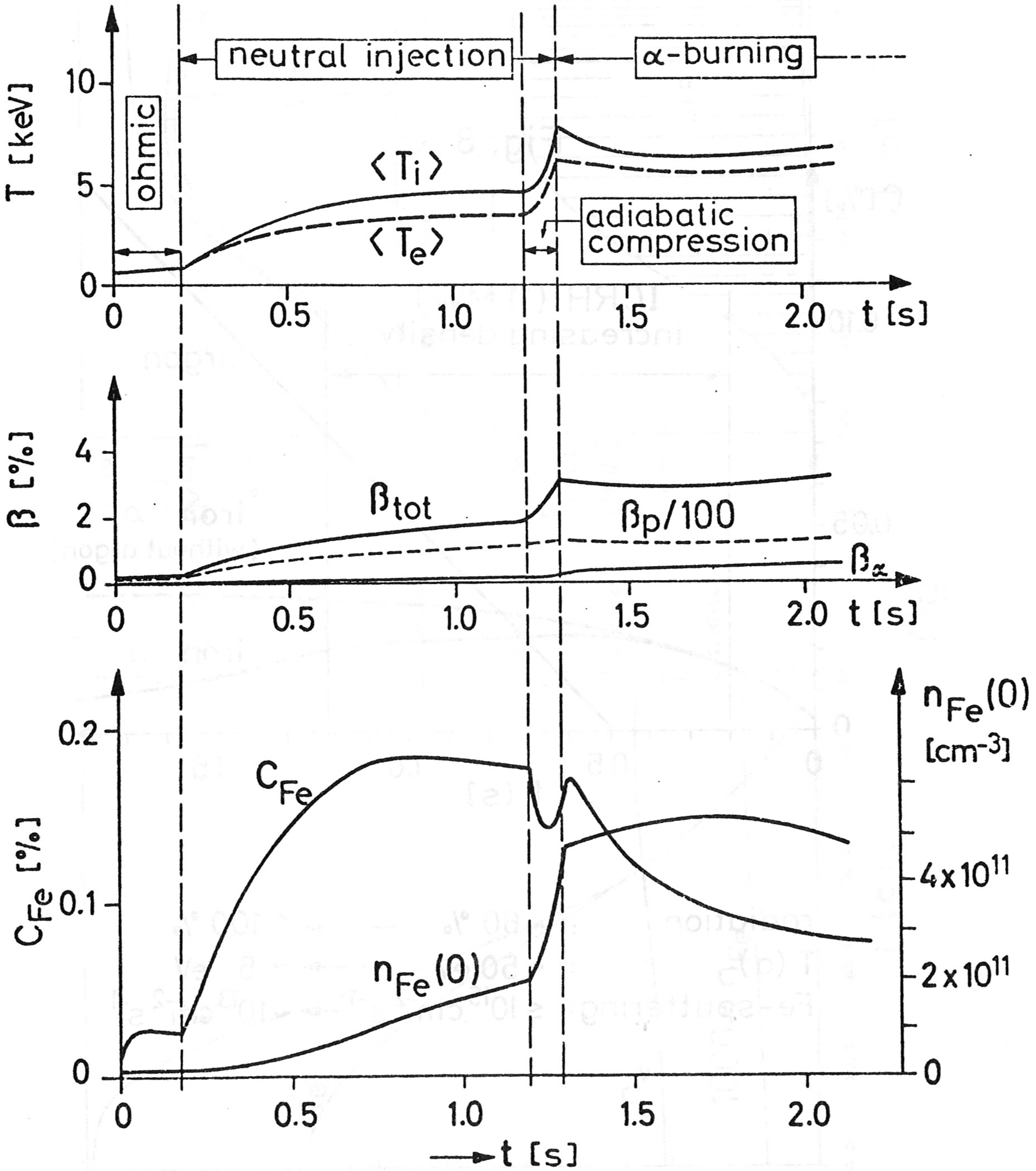

neutral injection
α-burning
ohmic
adiabatic compression
T [keV]
10
5
0
⟨Ti⟩
⟨Te⟩
0
0.5
1.0
1.5
2.0
t [s]
β [%]
4
2
0
βtot
βp/100
βα
0
0.5
1.0
1.5
2.0
t [s]
CFe [%]
0.2
0.1
0
CFe
nFe(0)
nFe(0)
[cm-3]
4x10^11
2x10^11
0
0
0.5
1.0
1.5
2.0
t [s]